Resonant x-ray diffraction as a tool to calculate mixed valence ratios: Application to Prussian Blue materials

Fabio Furlan Ferreira, Paulo R. Bueno, Grazielle O. Setti, David Giménez-Romero, José Juan García-Jareño et al.

Citation: Appl. Phys. Lett. **92**, 264103 (2008); doi: 10.1063/1.2952457
View online: http://dx.doi.org/10.1063/1.2952457
View Table of Contents: http://apl.aip.org/resource/1/APPLAB/v92/i26
Published by the AIP Publishing LLC.

Resonant x-ray diffraction as a tool to calculate mixed valence ratios: Application to Prussian Blue materials

Fabio Furlan Ferreira,[1,a)] Paulo R. Bueno,[2,a)] Grazielle O. Setti,[2] David Giménez-Romero,[3] José Juan García-Jareño,[3] and Francisco Vicente[3]
[1]*Laboratório Nacional de Luz Síncrotron, C. Postal 6192, Campinas, São Paulo 13083-970, Brazil*
[2]*Inst. de Química, Universidade Estadual Paulista, C. Postal 355, Araraquara 14800-900 São Paulo, Brazil*
[3]*Dept. de Química Física, Universitat de València, C/Dr Moliner, 50, Burjassot, València, 46100, Spain*

(Received 22 December 2007; accepted 5 June 2008; published online 2 July 2008)

An approach is proposed here to calculate mixed valence ratios in molecular compounds. Synchrotron x-ray powder diffraction experiments were conducted to determine the Fe^{+3}/Fe^{+2} ratio in Prussian Blue compounds, which were elected as an example of the use of this approach. As a result, a resonant x-ray diffraction measurement provided direct evidence that the vacant $[Fe(CN)_6]$ group was randomly absent from ~31% of the structure, which was indicated by structural differences caused by variations in the anomalous dispersion term. These findings are very important for a deeper understanding of the changes occurring in properties during *in situ* compositional variations. © *2008 American Institute of Physics*. [DOI: 10.1063/1.2952457]

The wide range of available x-ray wavelengths at synchrotron sources has made it feasible to conduct experiments in resonant x-ray diffraction. This is a well established technique for tuning x-ray energy close to an absorption edge to enhance the sensitivity of a particular element or to differentiate valence states of the resonant element.[1] On the other hand, it is also well known that choosing an incident wavelength far away from the absorption edge of the constituent elements renders the atomic scattering factor independent of the energy.[2] Now, if one chooses an incident wavelength close to the absorption edge of the constituent elements, the real and imaginary components of the anomalous dispersion term, f' and f'', respectively, become significant.[2] The energy and momentum dependency of the atomic scattering factor is generally expressed by $f(Q,E)=f_0(Q)+f'(E)+if''(E)$, where Q and E are the wave vector and the incident x-ray energy, respectively.[2]

Considering the aspects discussed in the previous paragraph, this paper proposes the use of the resonant x-ray tunability of a synchrotron source to perform x-ray diffraction experiments that can be used as a tool to calculate the mixed iron valence ratio, M^{+3}/M^{+2}, in molecular compounds. The effect of the resonant x-ray tunability is clearly visible by variations in the integrated intensity of some reflections, which, in fact, are related directly to differences in their structure factors. To illustrate the usefulness of the approach proposed here, a calculation was made of the mixed valence ratio, Fe^{+3}/Fe^{+2}, of a very classical molecular compound—Prussian Blue (PB) material. PB material, more specifically $K_hFe_k[Fe(CN)_6]_l\cdot mH_2O$ (determined here as $K_{2.1}Fe_4[Fe(CN)_6]_3\cdot 14H_2O$), is a subclass of the hexacyanometallates, a hexacyanoferrate which is known to exhibit identical metal atoms existing in different spin and/or oxidation states.[3,4]

Furthermore, although the mixed valence ratio is a crucial information regarding the real stoichiometry of this kind of compound, providing a quantitative understanding of superexchange interactions and tunneling of magnetism and coloration properties,[5] it has never before been reported.

Therefore, high-intensity synchrotron x-ray powder diffraction data were collected at the x-ray powder diffraction (D10B-XPD) beamline[6] of the Brazilian Synchrotron Light Laboratory (LNLS, Campinas, Brazil). X rays of $\lambda_1=1.378\,62(2)$ Å, $\lambda_2=1.741\,56(2)$ Å, and $\lambda_3=1.761\,40(8)$ Å wavelengths were selected by a double-bounce Si(111) monochromator. A vertically collimated beam was used in the experiments on a spot of ~1 mm (vertical) × ~2 mm (horizontal) in the sample's position in order to increase the resolution of the beamline's energy, which was ~1.5 eV at wavelengths near the Fe absorption edge (λ_2 and λ_3). The diffracted beam was analyzed with a pyrolitic graphite HOPG(002) and detected with a NaI(Tl) scintillation counter. The incoming beam was also monitored by a scintillation counter for normalization of the decay of the primary beam. The powder sample was loaded into a 0.5 mm diameter borosilicate glass capillary and data were recorded at room temperature for 10 s at each 2θ in steps of 0.06° from 10° to 90°.

The PB powder diffraction patterns were simultaneously refined by the Rietveld method using the general structure analysis system[7] (GSAS) software program and its graphical user interface, EXPGUI.[8] The space group was $Fm\bar{3}m$ and the lattice parameter $a=10.1780(7)$ Å. The model proposed by Herren *et al.*,[9] obtained from a neutron diffraction profile analysis, was considered as the initial structural model and was able to provide a precise analysis of the PB-type compound's main structure. In this model, Fe^{+3} ions occupy the 4*a* sites (0,0,0), Fe^{+2} ions occupy the 4*b* sites $(\frac{1}{2},\frac{1}{2},\frac{1}{2})$, and C, N, K and one of the three O^{-2} ions occupy the 24*e* sites $(x,0,0)$, with $x\sim0.30$, 0.19, 0.33, and 0.22, respectively. The other two O^{-2} ions occupy the 8*c* $(\frac{1}{4},\frac{1}{4},\frac{1}{4})$ and 32*f* (x,x,x) sites, with $x\sim0.32$. The main difference between the model proposed by Herren *et al.*[10] and the one used by us is the inclusion of the K ions in the structure. The background was fit using a 24-term shifted Chebyschev function. The peak

[a)]Authors to whom correspondence should be addressed. Electronic addresses: prbueno@iq.unesp.br and furlan@lnls.br.

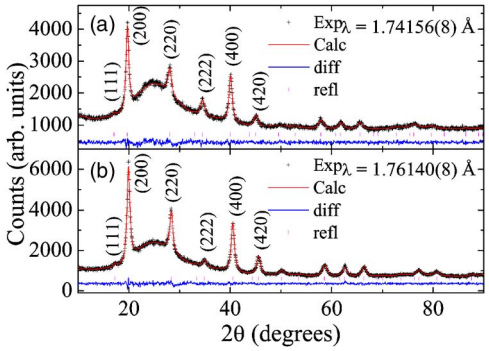

FIG. 1. (Color online) (a) Ratio of the normalized integrated intensities of the different wavelengths used, showing the effect on the various Bragg reflections. Dashed lines serve to guide the eyes. (b) Fe *K*-edge absorption of the PB sample. The horizontal arrows indicate that two of the wavelengths (λ_1 and λ_3) are outside the limits used for this measurement. The vertical arrow shows the position of the other wavelength (λ_2).

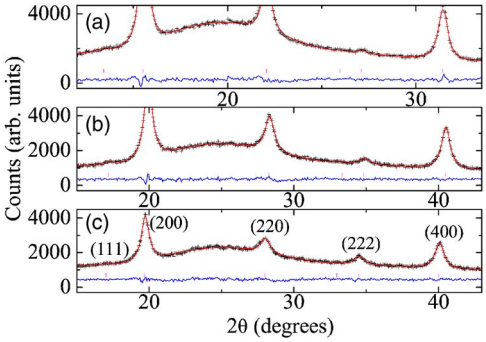

FIG. 2. (Color online) Rietveld refinements of the $K_h Fe_k[Fe(CN)_6]_l \cdot mH_2O$ structure measured at two distinct wavelengths: (a) $\lambda_2 = 1.741\,56(2)$ Å and (b) $\lambda_3 = 1.761\,40(8)$ Å. (+) observed, (red line) calculated, (blue line) difference, and (magenta symbol) Bragg reflections. A few selected indexed reflections are indicated.

profile was modeled by a pseudo-Voigt profile function as parametrized by Thompson *et al.*[10] with asymmetry corrections by Finger *et al.*[11] and microstrain anisotropic broadening terms by Stephens.[12]

In the PB system, the only edge which allows for an x-ray wavelength that can be used for hard x-ray diffraction is the Fe *K* edge. Due to the characteristics of the scattering theory, data collected at ~73 eV below the Fe *K* edge (7.112 keV=1.7433 Å) were used to minimize the imaginary anomalous scattering term (f'') of iron. In order to differentiate the ratio between Fe^{+2} and Fe^{+3} ions, thus taking into account the fact that the Fe^{+2} would undergo absorption, a resonant x-ray diffraction experiment was performed between the absorption edges of the two Fe ions (above the Fe^{+2} edge and below the Fe^{+3} one), which are separated by ~5 eV,[13] as later evidenced by us and shown in the inset of Fig. 3. With this condition, the dependence of the atomic scattering factor of the Fe^{+3} was enhanced in contrast to the Fe^{+2}, thus indicating a certain vacancy in some crystallographic sites, as will be discussed below.

Figure 1 shows the Rietveld refinements of the same PB sample measured at two distinct wavelengths: $\lambda_2 = 1.741\,56(2)$ Å and $\lambda_3 = 1.761\,40(8)$ Å. The goodness-of-fit indicator χ^2 and *R* factors, R_{wp} and $R_F{}^2$,[14] for both refinements were, respectively, $\chi^2 = 1.23$, $R_{wp\_\lambda 2} = 2.84\%$, and $R_F{}^2{}_{\_\lambda 2} = 3.47\%$, and $R_{wp\_\lambda 3} = 2.88\%$, and $R_F{}^2{}_{\_\lambda 3} = 1.81\%$. Although a significant difference in $R_F{}^2$ values arose, the validity of the structural model cannot be disregarded. This can also be evaluated by a visual inspection of the fitting. The complete structural model is presented elsewhere.[15] To account for variations in the integrated intensities of the different x-ray diffractograms due to resonant scattering, the FPRIME software,[16] which is part of the GSAS program,[7] was used to calculate the scattering factors of the constituent elements of the sample and to make corrections due to absorption. The expression of the integrated intensity in powder diffraction can be expressed by $I_{hkl} = K \times p_{hkl} \times L_\theta \times P_\theta \times A_\theta \times T_{hkl} \times E_{hkl} \times |F_{hkl}|^2$, where *K* is the scale factor, i.e., it is a multiplier required to normalize experimentally observed integrated intensities with absolute calculated intensities, p_{hkl} is the multiplicity factor, L_θ is the Lorentz multiplier, P_θ is the polarization factor, A_θ is the absorption multiplier, T_{hkl} is the preferred orientation factor, E_{hkl} is the extinction multiplier, and F_{hkl} is the structure factor. Details of all these terms can be found in Ref. 17. The last term in the expression of the integrated intensity, $|F_{hkl}|^2$, the structure factor, is expressed by

$$\mathbf{F}_{hkl} = \sum_{j=1}^{n} g^j t^j(s) f^j(s) \exp[2\pi \mathbf{i}(hx^j + ky^j + lz^j)],$$

where $\mathbf{F}_{hkl}$ is the structural amplitude of a Bragg reflection with *hkl* indices, *n* is the total number of atoms in the unit cell and *n* includes all symmetrically equivalent atoms, *s* is $\sin\theta_{hkl}/\lambda$, g^j is the occupation of the *j*th atom ($g^j = 1$ for a fully occupied site), t^j is the temperature factor, which describes thermal motions of the *j*th atom, and $f^j(s)$ is the atomic scattering factor describing the interaction of the incident wave with a specific type of atom as a function of $\sin\theta_{hkl}/\lambda$ for x rays or electrons, and is simply f^j (i.e., independent of $\sin\theta_{hkl}/\lambda$) for neutrons; $\mathbf{i} = \sqrt{-1}$.[17]

Initially, we took into account the f' value for each iron ion as being equal to the scattering factor of the neutral atom for each wavelength. The scattering factors of the C, N, O, and K atoms are much smaller than the Fe and were not considered to vary. Refinements of the f' terms for the Fe^{+2} and Fe^{+3} ions yielded the values of −3.4(2) and −4.1(2) for λ_3 and −8.0(3) and −9.7(3) for λ_2, respectively. As discussed in the literature concerning the effects of ion contrast in x-ray diffraction experiments, the patterns are more sensitive to f', and the Kramers–Kronig[18] transformation looks like a Lorentzian convolution filter, which makes the decrease in f' stable enough.[19] Also, a comparison of the refined values with others described in the literature[20] for magnetite indicates compatibility, thus confirming their accuracy. This is an interesting result because if one considers the fact that the number of electrons decreases, the same effect should occur with the intensity of the peaks. That is true for most of them, but in the specific case of the (222) reflection, its integrated intensity is increased. Considering that the absorption effects are the same for all the reflections, this higher integrated intensity is explained by the differences in the occupation of the *j*th site. It is known from the structural model considered[9] that the PB structure has ~25% missing Fe^{+2} ions (in fact, it is the $Fe[(CN)_6]$ group that is vacant). It should be noted that, according to the structural model, Fe^{+2} and Fe^{+3} ions do not occupy the same crystallographic site. The vacant $Fe[(CN)_6]$ group is occupied by water molecules

TABLE I. Integrated intensities, normalized with respect to the (200) one, of the three distinct wavelengths: $\lambda_1=1.378\,62(2)$ Å, $\lambda_2=1.741\,56(2)$ Å, and $\lambda_3=1.761\,40(8)$ Å.

h	k	l	$\lambda_1=1.378\,62$ Å	$\lambda_2=1.741\,56$ Å	$\lambda_3=1.761\,40$ Å
1	1	1	2.3	4.5	3.4
2	0	0	100	100	100
2	2	0	52.3	38.7	47.6
2	2	2	3.9	28.1	9.2
4	0	0	47.0	60.9	54.2
4	2	0	27.7	18.4	23.1

coordinated to the structure and K^+ ions to counterbalance the charge. What is more, this is a key point in the changeover on the properties during *in situ* compositional variation.[5] For the sake of clarity, Table I shows the normalized integrated intensities for some selected reflections extracted from the GSAS software used in Fig. 3.

Figure 2 shows a selected 2θ range of the x-ray diffractograms measured with (a) λ_1, (c) λ_2, and (b) λ_3, where the most intense reflections of PB lie. According to the literature,[21] the fact that the (111) reflection is not totally absent may be associated with a face-centered cubic lattice with Fe^{+3} ions located at the corners and at the center of the faces of the cubes and a partial occupation of the octahedral sites by Fe^{+2} ions. This is experimentally evidenced even in cases in which the wavelengths did not differentiate the two iron ions, i.e., in λ_1 and λ_3. Although the differences occur in the various reflections, the most prominent effect occurs in the (222) reflection. This is clearly evidenced in Fig. 3, which shows the normalized integrated intensities (which are proportional to the square of the modulus of the structure factor) for the different wavelengths used. This demonstrates that the vacant $[Fe(CN)_6]$ group can be evaluated in spite of a full-pattern Rietveld refinement to be located at particular sites in the structure. If the integrated intensity of a given reflection is known and the same sample is measured in at least two selected wavelengths, it is possible to dimension the vacant sites in a structure. The only requirement here is that the f' values of the different ions in each wavelength are known. In the present case, the Fe^{+3}/Fe^{+2} ratio, obtained directly from the (222) reflection in Fig. 3 [i.e., the ratio between the measurement taken between the absorption edges (λ_2) of Fe^{+2} and Fe^{+3} and below the absorption edge of both iron ions (λ_3) to evaluate the contribution of Fe^{+2}], indicates that the vacant $[Fe(CN)_6]$ group is randomly absent from ~31% of the structure. This finding is consistent with a previous result obtained by a full-pattern Rietveld refinement.[15] The results reported here are very important for a deeper understanding of the changes occurring in properties during *in situ* compositional variations,[5] as has been evidenced elsewhere.[15]

In conclusion, it was shown that resonant x-ray diffraction analysis can be used as a tool to calculate the Fe^{+3}/Fe^{+2} ratio in a hexacyanoferrate material, thanks to the ability of resonant x-ray diffraction to enhance the sensitivity of one of the iron ions by tuning the wavelength above the Fe^{+2} absorption edge and below the Fe^{+3} one. This information is crucial for a thorough understanding of such compounds. The proposed approach is applicable to other hexacyametallates and to various other molecular compounds of mixed valences.

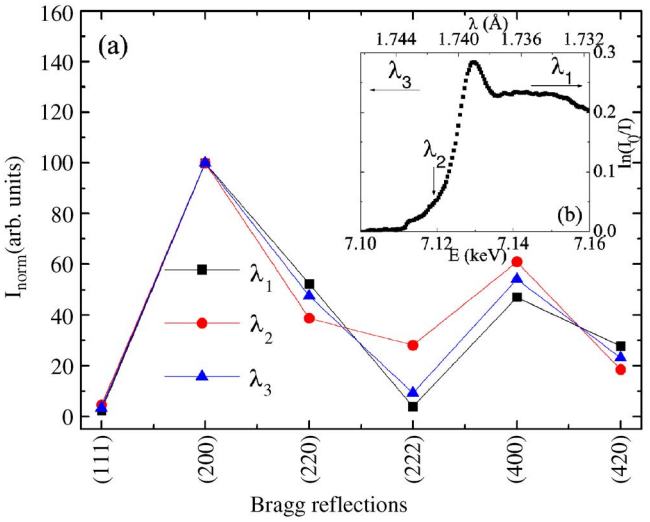

FIG. 3. (Color online) Rietveld refinements (selected regions) of the $K_hFe_k[Fe(CN)_6]_l \cdot mH_2O$ structure measured at three distinct wavelengths: (a) $\lambda_1=1.378\,62(2)$ Å, (b) $\lambda_2=1.761\,40(8)$ Å, and (c) $\lambda_3=1.741\,56(2)$ Å. (+) observed, (red line) calculated, (blue line) difference, and (magenta symbol) Bragg reflections. Various selected indexed reflections are indicated.

This work was supported by the São Paulo state research funding agency (FAPESP). We thank the LNLS for the use of its beam line. D.G.-R. acknowledges the financial support of the Generalitat Valenciana.

[1] G. Materlik, C. J. Sparks and K. Fisher, *Resonant Anomalous X-Ray Scattering: Theory and Applications* (Elsevier Science, Amsterdam, 1994).
[2] Y. Waseda, *Nature of Anomalous X-ray Scattering and Its Application to the Structural Analysis of Crystalline and Non-Crystalline Systems, in Anomalous X-ray scattering for Materials Characterization* (Springer, Berlin, 2002), p. 21.
[3] O. Sato, T. Iyoda, A. Fujishima, and K. Hashimoto, Science **272**, 704 (1996).
[4] N. R. de Tacconi, K. Rajeshwar, and R. O. Lezna, Chem. Mater. **15**, 3046 (2003).
[5] P. R. Bueno, D. Gimenez-Romero, C. Gabrielli, J. J. Garcia-Jareño, H. Perrot, and F. Vicente, J. Am. Chem. Soc. **128**, 17146 (2006).
[6] F. F. Ferreira, E. Granado, W. Carvalho, Jr., S. W. Kycia, D. Bruno, and R. Droppa, Jr., J. Synchrotron Radiat. **13**, 46 (2006).
[7] A. C. Larson and R. B. Von Dreele, Los Alamos National Laboratory Report No. LAUR 86-748, 2001.
[8] B. H. Toby, J. Appl. Crystallogr. **34**, 210 (2001).
[9] F. Herren, P. Fisher, A. Ludi, and W. Halg, Inorg. Chem. **19**, 956 (1980).
[10] P. Thompson, D. E. Cox, and J. B. Hastings, J. Appl. Crystallogr. **20**, 79 (1987).
[11] L. W. Finger, D. E. Cox, and A. P. Jephcoat, J. Appl. Crystallogr. **27**, 892 (1994).
[12] P. W. Stephens, J. Appl. Crystallogr. **32**, 281 (1999).
[13] A. Ide-Ektessabi, T. Kawakami, and F. Watt, Nucl. Instrum. Methods Phys. Res. B **213**, 590 (2004).
[14] B. H. Toby, Powder Diffr. **21**, 67 (2006).
[15] P. R. Bueno, F. F. Ferreira, D. Giménez-Romero, R. C. Faria, G. O. Setti, J. J. Garcia-Jareño, F. Vicente, C. Gabrielli and H. Perrot, J. Phys. Chem. C (unpublished).
[16] D. T. Cromer, J. Appl. Crystallogr. **16**, 437 (1983).
[17] V. K. Pecharsky and P. Y. Zavalij, *Fundamentals of Powder Diffraction and Structural Characterization of Materials* (Springer, Binghamton, NY, 2005).
[18] J. Als-Nielsen and D. McMorrow, *Elements of Modern X-ray Physics* (Wiley, Chichester, 2001).
[19] J. Lorimier, F. Bernard, J.-C. Niepce, N. Guigue-Millot, O. Isnard, and J.-F. Bérar, **36**, 301 (2003).
[20] R. J. Goff, J. P. Wright, J. P. Attfield, and P. G. Radaelli, J. Phys.: Condens. Matter **17**, 7633 (2005).
[21] A. Bleuzen, C. Lomenech, V. Escax, F. Villain, F. Varret, C. C. dit Moulin, and M. Verdaguer, J. Am. Chem. Soc. **122**, 6648 (2000).